Lifetime Measurements in ^{134}Pr and Chirality in Nuclei

Article · June 2006

23 authors, including:

Pavel Petkov
Horia Hulubei National Institute for R&D in Physics and Nuclear Engineering
225 PUBLICATIONS   **2,991** CITATIONS

SEE PROFILE

D.L Balabanski
Extreme Light Infrastructure - Nuclear Physics
396 PUBLICATIONS   **4,615** CITATIONS

SEE PROFILE

Giacomo de Angelis
INFN - Istituto Nazionale di Fisica Nucleare
882 PUBLICATIONS   **9,668** CITATIONS

SEE PROFILE

A. Gadea
Spanish National Research Council
711 PUBLICATIONS   **8,737** CITATIONS

SEE PROFILE

Some of the authors of this publication are also working on these related projects:

Project   gamma strenght functions View project

Project   Superheavy Elements View project

World Scientific
www.worldscientific.com

LIFETIME MEASUREMENTS IN ^{134}Pr AND CHIRALITY IN NUCLEI

D. TONEV, P. PETKOV* and D. L. BALABANSKI

Institute for Nuclear Research and Nuclear Energy,
Bulgarian Academy of Sciences, 1784 Sofia, Bulgaria
*mitko@lnl.infn.it

G. DE ANGELIS, A. GADEA, D. R. NAPOLI and N. MARGINEAN

INFN, Laboratori Nazionali di Legnaro, 35020 Legnaro (PD), Italy

A. DEWALD, P. PEJOVIC, A. FITZLER, O. MÖLLER and K. O. ZELL

Institut für Kernphysik der Universität zu Köln, 50937 Köln, Germany

S. BRANT

Department of Physics, Faculty of Sciences,
University of Zagreb, 10000 Zagreb, Croatia

S. FRAUENDORF

Department of Physics, University of Notre Dame, 46556 Indiana, USA

D. BAZZACCO, S. LENZI and S. LUNARDI

Dipartimento di Fisica, Università and INFN Sezione di Padova,
35131 Padova, Italy

P. BEDNARCZYK and D. CURIEN

Institut de Recherches Subatomique, 67037 Strasbourg, France

C. PETRACHE

Dipartimento di Fisica, Università di Camerino and INFN Perugia,
62032 Camerino, Italy

Q. ZHONG

Department of Nuclear Physics, China Institute of Atomic Energy,
102413, Peoples Republic of China

Y. H. ZHANG

Institute of Modern Physics, Chinese Academy of Sciences,
73000 Lanzhou, Peoples Republic of China

JING-YE ZHANG

Department of Physics and Astronomy, University of Tennessee,
37996 Knoxville, Tennessee, USA

Lifetimes of exited states in ^{134}Pr were measured be means of the recoil distance Doppler-shift and Doppler-shift attenuation techniques. The experiments were performed at IReS, Strasbourg using the EUROBALL IV spectrometer, in conjunction with the inner BGO ball and the Cologne coincidence plunger apparatus. Exited states in ^{134}Pr were populated in the fusion-evaporation reaction ^{119}Sn(^{19}F, 4n)^{134}Pr. Reduced transition probabilities in ^{134}Pr are compared to the predictions of the two quasiparticle+triaxial rotor and interacting boson fermion-fermion models. The experimental results do not support the presence of static chirality in ^{134}Pr underlying the importance of shape fluctuations. Only within a dynamical context the presence of intrinsic chirality in ^{134}Pr can be supported.

1. Introduction

Static chiral symmetries exist commonly in nature. Examples of this interesting phenomenon have been found in chemistry, biology, pharmacy and particle physics. Chirality has recently been proposed as a novel feature of rotating nuclei.[1−3] A spontaneous breaking of the chiral symmetry can take place for configurations where the angular momenta of the valence protons, valence neutrons and the core are mutually perpendicular. This can occur, for example, when the proton and neutron Fermi levels are located in the lower part of valence proton high-j (particle-like) and in the upper part of valence neutron high-j (hole-like) subshells, and the core is triaxial. Under such conditions the angular momenta of the valence particles are aligned along the short and long axes of the triaxial core, while the angular momentum of the rotational core is aligned along the intermediate axis. The non zero components of the total angular momentum on all the three axes can form either a left-handed or a right-handed set and therefore, the system manifests chirality.[2] Since the chiral symmetry is dichotomic, its spontaneous breaking by the axial angular momentum vector leads to doublets of closely lying rotational bands of the same parity.[1−3]

Pairs of bands possibly due to the breaking of the chiral symmetry have been found in a wide region of masses, namely A ∼ 105,[4−6] A ∼ 130,[7−11] A ∼ 190.[12] There is also a big interest from theoretical point of view to investigate the chiral phenomenon.[2,13−15] In the present work we will concentrate on the investigation of the nucleus ^{134}Pr shown to be the best candidate to express chirality.[2,3] The first example of two nearly degenerate bands with the same parity and spins has been reported for ^{134}Pr.[16,17] The two bands are displayed in Fig. 1. The degeneracy between levels of the same spin and parity is increasing with increasing spin and the bands cross above I > 15$\hbar$. In the context of chiral symmetry such a doublet of bands has been described within the framework of the particle-core coupling model[1,3] and the tilted-axis cranking model.[2] An alternative interpretation has been based on the interacting boson fermion-fermion model (IBFFM).[19] Here the energy degeneracy is also obtained but a different nature is attributed to the two bands. The yrast band is basically built on the ground state configuration of the triaxial core whereas the collective structure of the yrare band contains a large component of the γ-band and, with increasing angular momentum, of higher-lying collective core structures.
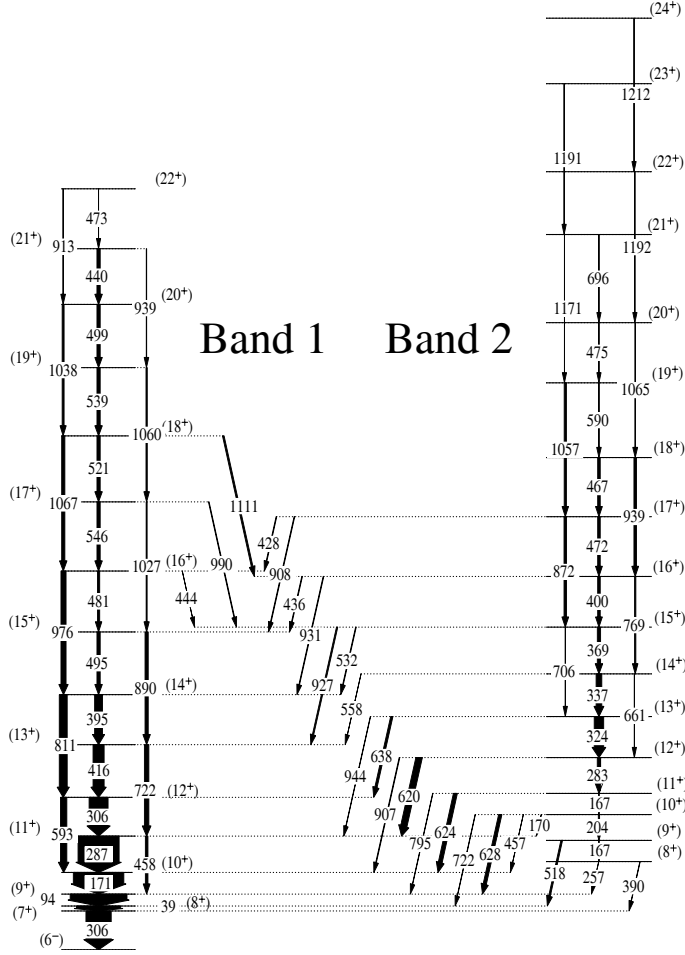
Fig. 1. Partial level scheme of ^{134}Pr from Ref. 18. Two nearly degenerate positive-parity bands, candidates for chiral partner bands, are indicated as Band 1 and Band 2.

In order to confirm or reject the hypothesis of nuclear chirality, next to establish the existence of almost degenerate rotational bands, it is necessary to measure also other observables and compare them to the model predictions. Critical experimental observables for the understanding of nuclear structure and for checking the reliability of theoretical models are the electromagnetic transition probabilities. The aim of the present work is to investigate the electromagnetic transition probabilities in the doublet bands of ^{134}Pr.

2. Experiment and Data Analysis

To populate excited states in ^{134}Pr using the recoil distance Doppler-shift (RDDS) and Doppler shift attenuation (DSA) methods, the fusion-evaporation reaction

^{119}Sn(^{19}F, 4n)^{134}Pr at beam energies of 87 and 83 MeV, respectively, was used. The beam was delivered by the Vivitron accelerator at IReS in Strasbourg. For the RDDS measurement, the target consisted of 0.5 mg/cm^2 ^{119}Sn foil enriched to 89.8%. It was evaporated on a 1.8 mg/cm^2 ^{181}Ta foil facing the beam. A 6.0 mg/cm^2 gold foil was used to stop the recoils which were leaving the target with a mean velocity of 0.98(2)% of the velocity of light, c. The target consisted of 0.7 mg/cm^2 ^{119}Sn evaporated on a 9.5 mg/cm^2 ^{181}Ta backing used to stop the recoils. The γ-rays deexciting the recoiling ^{134}Pr nuclei were detected using the EUROBALL IV[20] detector array composed of 26 clover and 15 cluster Ge detectors and an inner BGO (Bismuth Germanate) ball. The cluster and clover detectors of EUROBALL were grouped into 10 rings corresponding to approximately the same polar angle with respect to the beam axis. The trigger condition for data acquisition was set such that events were recorded when at least three γ-rays in the Ge cluster or clover segments and three segments of the inner ball fired in prompt coincidence. Under such trigger conditions, the yield of ^{134}Pr was estimated to be 28% of the total cross-section. Gain matching and efficiency calibration of the Ge detectors were performed using ^{133}Ba, ^{152}Eu and ^{56}Co radioactive sources. A standard add-back correction for Compton scattering was applied. The data were sorted into γ-γ coincidence matrices. For the RDDS measurement, data were taken at 20 target-to-stopper distances ranging from electrical contact to 2500 μm. Some of the investigated transitions have low energies, and since v/c is 0.98(2)%, the resulting Doppler-shift is relatively small. For this reason, in the analysis, only detectors with good resolution were selected in order to obtain better line-shapes. For the RDDS case the normalization of the data taken at different target-to-stopper distances was performed using coincidence events corresponding to pairs of strong transitions. Examples of spectra taken at different distances for two γ-ray transitions in ^{134}Pr are shown in Fig. 2.

For the analysis of the RDDS data, the standard version of the Differential decay-curve method (DDCM)[21] has been employed, with gates set on both shifted (S) and unshifted (U) components of a transition depopulating levels below the level of interest. For each flight time t, a lifetime value τ for the level of interest is calculated by directly using the areas of the U or S peaks of a transition depopulating the investigated level and of the directly feeding transitions. A lifetime value is derived at each distance and the final result for τ is determined as an average of such values within the sensitivity region of the data. More details about the DDCM applied to RDDS measurements can be found in Refs. 21, 22 For the analysis of the DSAM data, we performed a Monte-Carlo simulation of the slowing-down histories of the recoils using a modified[23,24] version of the program. DESASTOP[25] The analysis of the lineshapes was carried out according to the DDCM for treating DSAM data.[22,23] Complementary details about the data analysis are presented in a forthcoming paper.[26]
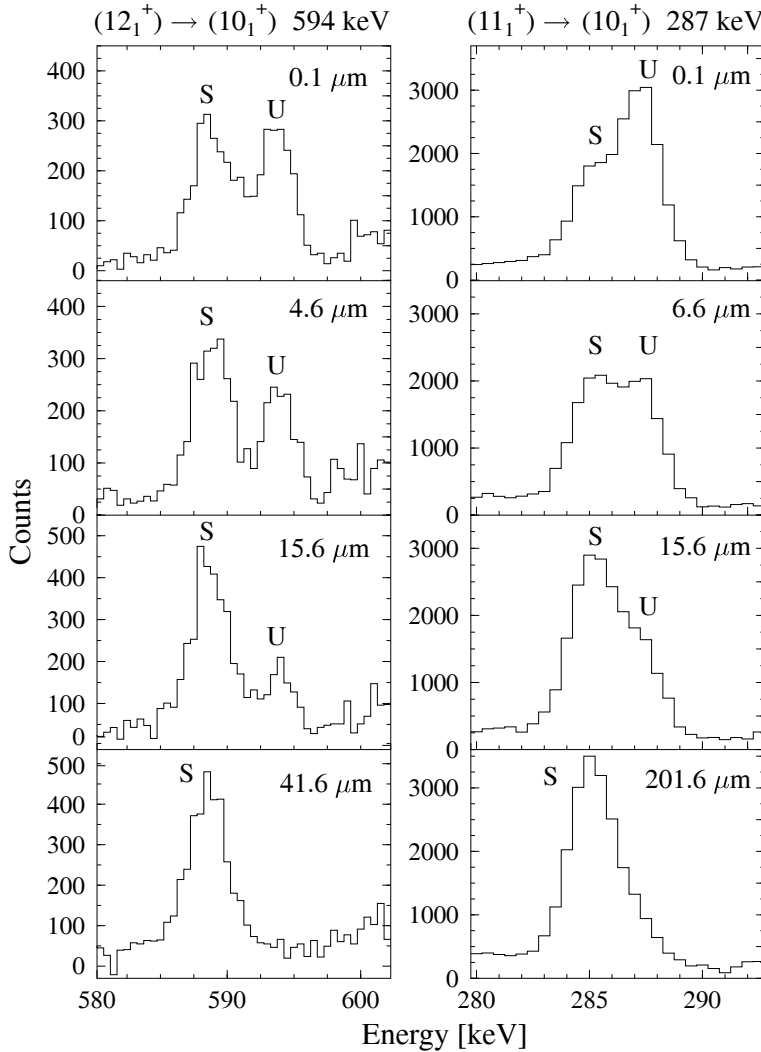
$(12_1^+) \rightarrow (10_1^+)$ 594 keV $(11_1^+) \rightarrow (10_1^+)$ 287 keV

Fig. 2.   Gated γ-ray spectra of ^{134}Pr taken at four different distances. The summed spectra from all detectors positioned at the backward angle of 137.60° with respect to the beam axis are shown. On the right-hand side, the shifted and unshifted components of the $11_1^+ \rightarrow 10_1^+$ transition are presented, on the left-hand side, the shifted and unshifted components of the $12_1^+ \rightarrow 10_1^+$ transition are shown.

3. Results and Discussion

The lifetimes of the levels with I$^\pi$ from 10_1^+ to 18_1^+ and with I$^\pi$ from 13_2^+ to 17_2^+ have been deduced.[27] Except for the lifetime of the I$^\pi$ = 10_1^+ level,[28] all the others are determined for the first time. We observe an excellent agreement with the lifetime value for the I$^\pi$ = 10_1^+ state reported in Ref. 28. The results for lifetime values are reported in the work.[27]

Almost all branching ratios reported in Ref. 16 were revised. The clover rings of Euroball form a highly efficient Compton polarimeter. We confirmed that the delayed component of the 306 keV doublet has an E1 character as already reported by Roberts *et al.*[29] On the basis of DCO[16] and linear polarization analysis, a M1 character with a negligible E2 component was assigned to the $\Delta I = 1$ intraband transitions. The $\Delta I = 2$ intraband and interband transitions show an E2 character. Details of the lifetime analysis, branching ratios and linear polarizations coefficients will be reported in a forthcoming publication.[26]

Reduced transition probabilities obtained from the present experiment are reported in the work[27] as well as they are shown in Fig. 3. Within the experimental uncertainties, the B(M1) values in both partner bands behave similarly and point to relatively strong transition strengths. In contrast, the intraband B(E2) strengths within the two bands differ. In the angular-momentum region where the almost degeneracy of the energy levels of the two bands occurs ($I^\pi = 14^+ - 19^+$), the B(E2) values for Band 1 are a factor 2 to 3 larger than those of Band 2. The B(M1)/B(E2) ratios obtained from the lifetime data are in a good agreement with the results extracted from intensity values reported in Ref. 16 and differ only for the $I^\pi = 13_1^+$ and 15_1^+ states from the values reported in Ref. 18 In all measurements the corresponding B(M1)/B(E2) ratios for the two bands are different. The staggering in Band 1 reported in Ref. 18 is not observed in our data as well as in the data of Ref. 16 Our results are incompatible with the pure chiral picture (static chirality) where the intraband B(E2) transition strengths must be almost equal.[1,30] Such a finding points to the fact that the limit of static chirality is not reached in ^{134}Pr and the nucleus stays in a very soft vibrational regime.

In order to investigate the effects of the shape fluctuations we have compared the experimental transition strengths of the two bands with calculated ones by means of the two quasiparticle + triaxial rotor model (TQPTR) as described in[1,31] and by the IBFFM.[19] For the TQPTR, the ratios between the moments of inertia have been calculated by cranking about the three principal axes using the parameters reported in Ref. 2, which gave $\mathcal{J}_s : \mathcal{J}_i : \mathcal{J}_l = 1.52 : 3.55 : 1$. In the IBFFM calculation, the proton and neutron were coupled to the triaxial core as described in Ref. 19 Both descriptions include the coupling between the odd particles and the even-even core in a similar way, taking into account the partial filling of the $h_{11/2}$ shells. In the TQPTR model, a rigid triaxial shape is assumed for the core and the orientation in space is the only core degree of freedom. The IBFFM takes into account the deformation of the core as an additional degree of freedom. As discussed in,[19] a cubic term had to be added to the standard IBA Hamiltonian in order to reproduce the energy spectra of ^{134}Pr and its even-even isobar ^{134}Ce. This term generates a triaxial equilibrium deformation. The fluctuations of the shape around this value are taken into account and their magnitude is fixed by adjusting the parameters for the IBA Hamiltonian to the data for ^{134}Ce. The results of both calculations are shown in Fig. 3. The comparison with the experimental data show a clear disagreement with the TQPTR results whereas a much better matching is

found with the IBFFM calculation. Such result indicates that shape fluctuations are an essential ingredient for the proper description of the structure of the two bands. The IBFFM could take into account the possibility that the angular momenta of the proton, neutron and core in odd-odd nucleus find themselves in the favorable geometry, as if they would be in the equivalent triaxially deformed rotor. This we will call in the following "dynamic chirality". The calculation presented in Ref. 26 will show that such possibility is present, but it is far from being dominant. The condition for the appearance of twin bands with wave functions realistic enough to reproduce the electromagnetic decay of the bands, is that the core is a γ-unstable rotor whose effective γ is in the range of triaxial values.

It is interesting to note that the difference of the transition strengths of the two bands is larger, and the theoretical values are closer to the experimental B(E2) values in the IBFFM calculation than in the TQPTR one. This fact supports the interpretation of Ref. 19 where the yrast band contains predominantly the ground state configuration of the triaxial core whereas the yrare band contains a major component of the γ-band. Such interpretation does not necessarily contradict the chiral interpretation, because the in the TQPTR calculations of Ref. 7 a similar composition was found.

In the chiral interpretation the eigenstates of the Hamiltonian representing the two observed bands can be described as linear combinations of the wave functions in the left-handed and right-handed sectors. In the case of static chirality the overlap between the wave functions in the two sectors is weak. Because such coupling represents the tunneling between the two chiral configurations, the matrix elements of the electromagnetic transition operators between the two chiral sectors are expected to be very small. Since the left- and right-handed components enter with equal weight into the two eigenstates, which differ only in the relative phase of the mixing amplitudes, the transition matrix elements of the two doublet bands have to be equal. In the case of dynamic chirality, the overlap between the wave functions of the two sectors is large. In such a condition there are large matrix elements of the transition operators that connect the left- to the right-handed sector. Due to orthogonality, these matrix elements enter the transition matrix elements of the eigenstates with opposite sign and make the transition strengths of the two doublet bands different.

The TQPTR calculation shows a transition from dynamic to static chirality with increasing spin. Below $I^\pi = 12^+$, the angular momentum vector oscillates between the left- and right-handed sectors, separated by the plane defined by the short and long axes(s-l). The two bands are well separated, representing the ground and first excited states of this chiral vibration.[17] Above $I^\pi = 12^+$, the angular momentum increases by adding core angular momentum perpendicular to the s-l-plane. This reduces the probability of the angular momentum vector to be near the s-l-plane, which makes the electromagnetic transition matrix elements between the two sectors small. Static chirality is approached, which is reflected by the two partner bands coming close together. The B(E2) values indicate that there is still a substantial
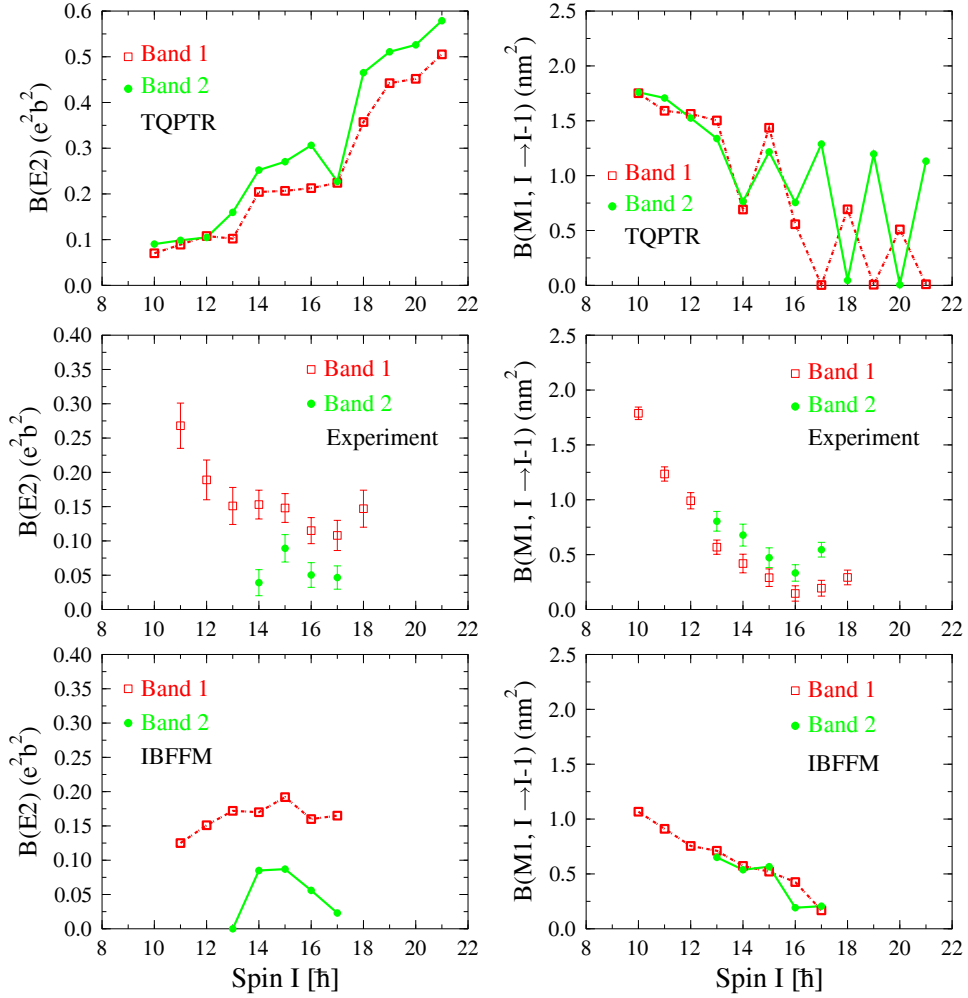
Fig. 3. Experimentally determined and theoretically calculated B(E2) and B(M1) transition strengths in chiral candidate bands of ^{134}Pr. In the upper panels are presented the results of TQPTR calculations. In the second row, the experimental B(E2) and B(M1) values for transitions in Band 1 and Band 2 are displayed. In the panels on bottom are presented the predictions of the IBFFM.

tunneling between the two sectors. In the IBFFM model, the fluctuations of the triaxiality parameter γ around its mean value of 30° admix near-axial shapes, which are achiral. This additional left-right coupling strongly increases the difference between the intraband B(E2) values. A pronounced staggering of the B(M1) values appears above $I^\pi = 12^+$ in the TQPTR model. An explanation for this staggering was given in Ref. 30 for the symmetric case where the angular momenta of the proton and the neutron hole are equal, the moments of inertia of the l- and s-axes are equal, and the left-right transition matrix element is negligible. Our TQPTR

calculation does not strictly obey these conditions, mainly because the microscopic moments of inertia of the long and short axes are different. The staggering is absent in the data as well as in the results of the IBFFM calculations, which indicates that the additional left-right coupling caused by the shape fluctuations cancels the staggering effect forseen in Ref. 30.

The assumption of a constant deformation of $\gamma = 30°$ in the TQPTR gives increasing B(E2) transition strengths as a function of spin, which is in contrast to the observed trend. Such an increase of the B(E2) transition strengths is directly related to the chiral geometry, which at low spins requires that the rotational axis lies in the plane defined by the short and long axes of the core, with an angle of 45° with respect to both of them. In such a situation the B(E2) values are equal to zero. With increasing spin the angular momentum moves out of the plane which correspondingly increases the B(E2) values. For axial shape instead the same geometry gives rise to large B(E2) values. Therefore, the admixture of near axial shapes will increase the B(E2) values at low spin, which results in the almost constant values seen in Fig. 3 and foreseen by the IBFFM calculations.

Our conclusions are supported by the recently published work[32] where the authors have critically analyzed the observed properties of chiral candidate bands in ^{134}Pr. Lifetime measurements for ^{132}La also put in question existence of chiral bands in ^{132}La.[11]

4. Conclusions

In summary, our lifetime measurements and the theoretical analysis do not support static chirality in ^{134}Pr, as suggested on the basis of the similar energies of the two positive parity bands.[1] The experimental B(E2) values are larger in Band 1 than in Band 2 whereas the B(M1) values are slightly larger in Band 2 than in Band 1. The experimental difference between the B(E2) values cannot be reproduced assuming a rigid triaxial shape (TQPTR) which would also result in a pronounced staggering of the B(M1) values not found in the experimental data. The experimentally observed transition matrix elements can be reproduced by taking into account the fluctuations of the nuclear shape (IBFFM). This means that the chirality in ^{134}Pr if existing has mainly a dynamical character, the nuclear system fluctuating between chiral and achiral configurations, which couples the two sectors and generates the differences in the transition rates. Thereby the coupling due to shape fluctuations seems to play a central role. However, it may also indicate that the coupling of the two quasiparticles to the shape degrees of freedom is the prominent mechanism.

the US Department of Energy by the contract numbers DE-FG02-95ER40934 and DE-FG02-96ER40983.

References

1. S. Frauendorf and J. Meng, *Nucl. Phys. A* **617** (1997) 131.
2. V. I. Dimitrov, S. Frauendorf and F. Dönau, *Phys. Rev. Lett.* **84** (2000) 5732.
3. K. Starosta, T. Koike, C. J. Chiara, D. B. Fossan and D. R. LaFosse, *Nucl. Phys. A* **682** (2001) 375c.
4. C. Vaman *et al.*, *Phys. Rev. Lett.* **92** (2004) 032501.
5. J. Timar *et al.*, *Phys. Lett. B* **598** (2004) 178.
6. P. Joshi *et al.*, *Phys.Lett. B* **595** (2004) 135.
7. K. Starosta *et al.*, *Phys. Rev. C* **65** (2002) 044328.
8. S. Zhu *et al.*, *Phys. Rev. Lett.* **91** (2003) 132501.
9. G. Rainovski *et al.*, *Phys. Rev. C* **68** (2003) 024318.
10. A. A. Hecht *et al.*, *Phys. Rev. C* **68** (2003) 054310.
11. J. Srebrny *et al.*, *Acta Phys. Polonica B* **36** (2005) 1063.
12. D. L. Balabanski *et al.*, *Phys. Rev. C* **70** (2004) 044305.
13. J. Peng, J. Meng and S. Q. Zhang, *Phys. Rev. C* **68** (2003) 044324.
14. P. Olbratowski, J. Dobaczewski, J. Dudek and W. Plóciemmik, *Phys. Rev. Lett.* **93** (2004) 052501.
15. J. Peng, J. Meng, S. Q. Zhang and S.-G. Zhou, *Phys. Rev. C* **73** (2006) 037303.
16. C. M. Petrache *et al.*, *Nucl. Phys. A* **597** (1996) 106.
17. K. Starosta *et al.*, *Phys. Rev. Lett.* **86** (2001) 971.
18. K. Starosta, in *Nuclei at the Limits*, ed. by T. L. Khoo and D. Seweryniak, *AIP Conf. Proc.* **764** (2005) 77.
19. S. Brant, D. Vretenar and A. Ventura, *Phys. Rev. C* **69** (2004) 017304.
20. J. Simpson, *Z. Phys. A* **358** (1997) 139.
21. A. Dewald, S. Harissopulos and P. von Brentano, *Z. Phys. A* **334** (1989) 163.
22. G. Böhm, A. Dewald, P. Petkov and P. von Brentano, *Nucl. Instrum. Methods Phys. Res. A* **329** (1993) 248.
23. P. Petkov *et al.*, *Nucl. Phys. A* **640** (1998) 293.
24. P. Petkov, D. Tonev, J. Gableske, A. Dewald, T. Klemme and P. von Brentano, *Nucl. Instrum. Methods Phys. Res. A* **431** (1999) 208.
25. G. Winter, *Nucl. Instrum. Methods* **214** (1983) 537.
26. D. Tonev *et al.*, to be published.
27. D. Tonev *et al.*, *Phys. Rev. Lett.* **96** (2006) 052501.
28. T. Klemme *et al.*, *Phys. Rev. C* **60** (1999) 034301.
29. S. P. Roberts *et al.*, *Phys. Rev. C* **67** (2003) 057301.
30. T. Koike, K. Starosta and I. Hamamoto, *Phys. Rev. Lett.* **93** (2004) 172502.
31. I. Ragnarsson and P. Semmes, *Hyperfine Interactions* **43** (1988) 425.
32. C. M. Petrache, G. B. Hagemann, I. Hamamoto and K. Starosta, *Phys. Rev. Lett.* **96** (2006) 112502.